

Novel Near-Infrared Fluorescence-Guided Surgery With Vesicular Stomatitis Virus for Complete Surgical Resection of Osteosarcomas in Mice

Tomohiko Sakuda,¹ Tadahiko Kubo,¹ Muhammad Phetrus Johan ^{1,2} Taisuke Furuta,¹ Takemasa Sakaguchi,³ Mahito Nakanishi,⁴ Mitsuo Ochi,¹ Nobuo Adachi¹

¹Department of Orthopaedic Surgery, Graduate School of Biomedical and Health Sciences, Hiroshima University, 1-2-3 Kasumi, Minami-ku, Hiroshima 734-8551, Japan, ²Department of Orthopedic and Traumatology, Faculty of Medicine, Hasanuddin University, Tamalanrea Makassar, Indonesia, ³Department of Virology, Graduate School of Biomedical and Health Sciences, Hiroshima University, Minami-ku, Hiroshima, Japan, ⁴National Institute of Advanced Industrial Science and Technology (AIST), Tsukuba, Ibaraki, Japan

Received 2 July 2018; accepted 20 February 2019

Published online in Wiley Online Library (wileyonlinelibrary.com). DOI 10.1002/jor.24277

ABSTRACT: Attempts have been made to visualize tumor cells intraoperatively with fluorescence guidance. However, the clear demarcation and complete tumor resection have always been a challenging task. To address this, we have developed a novel fluorescence bioimaging system with vesicular stomatitis virus (VSV) incorporating Katushka, near-infrared fluorescent protein. VSV is tumor-specific owing to the deficiency of antiviral interferon signaling pathways in tumor cells. We aimed to evaluate the tumor specificity of the recombinant VSV-Katushka (rVSV-K) in osteosarcoma cells and to assess the feasibility of complete tumor resection by the rVSV-K fluorescence guidance. In *in vitro* experiments, mouse and human osteosarcoma cell lines and normal human mesenchymal stem cells were infected with rVSV-K and observed by fluorescence microscopy. Near-infrared fluorescence was observed only in osteosarcoma cells, even at a low-concentration of virus infections. In *in vivo* experiments, mouse osteosarcoma (LM8) cells were transplanted subcutaneously into the back of immune-competent mice to produce an osteosarcoma, which was then injected with rVSV-K. The areas emitting fluorescence were resected using a bioimaging system. The distance between the surgical and tumor margins of the fluorescence-guided resection with rVSV-K group was significantly larger than that of the non-guided resection groups. The local recurrence rate was significantly lower in the fluorescence-guided resection with rVSV-K group than in the non-guided resection groups. The distant metastasis rate and average survival rate were not significantly different between all groups. These results suggest that the rVSV-K is specific to osteosarcoma cells and enables complete tumor resection of osteosarcomas in mice. © 2019 Orthopaedic Research Society. Published by Wiley Periodicals, Inc. *J Orthop Res* 37:1192–1201, 2019.

Keywords: vesicular stomatitis virus; katushka; osteosarcoma; fluorescence-guided resection

The standard treatment for osteosarcoma consists of surgery with adjuvant chemotherapy.^{1,2} Surgery can include resection of the muscles, tendons, ligaments, bones, and joints.³ The presence of residual cancer cells in the surgical area is predictive of local recurrence and survival. Local recurrence after adjuvant therapy is most resistant to treatment.^{4–6} Moreover, it is unclear whether local recurrence affects overall survival in addition to affecting adjuvant chemotherapy.^{5–8} Thus, it should be considered in the outcome of the surgical management of osteosarcoma.

The basic principle of malignant bone and soft tissue tumor resection is wide resection *en bloc* together with the surrounding normal tissue. Tumor resection margins are difficult to identify intraoperatively and must be estimated to some extent by the preoperative magnetic resonance imaging or computed tomography. However, these imaging modalities are insufficient to accurately identify the tumor margin intraoperatively.

Fluorescence imaging is a promising method for cancer screening and surgical resection.⁹ The first use of fluorescence imaging in surgery dates back to 1948

with the use of intravenous fluorescein to enhance intracranial neoplasms during neurosurgery.¹⁰ Since then, additional fluorescent substances have been studied, which include green fluorescent protein (GFP),¹¹ indocyanine green,¹² and quantum dots.¹³

The delivery of a fluorescent substance to tumor cells has been problematic and constitutes a major hurdle to the widespread clinical application of fluorescence imaging. Fluorescent substances are not actively taken up by tumor cells and fluorescence imaging is limited by the strong absorbance and scattering of light by the surrounding tissue.¹⁴ The development of a biologic carrier of fluorescent substances to specifically identify tumor cells *in vivo* would increase the accuracy of tumor resection. This paradigm requires an easily administered agent with high specificity for many cancer types and low affinity for non-cancerous tissues.¹⁴

Attempts have been made to visualize malignant tumor cells intraoperatively using tumor-specific viruses that selectively replicate in cancer cells and rarely infect normal cells.^{15–18} A virus-based tumor labeling method has been developed in preclinical studies for fluorescence-guided surgery. Most of these studies used an engineered DNA virus such as telomerase-dependent adenovirus^{15–18} or telomerase-dependent herpes simplex virus¹⁴ for malignant tumor detection. The vesicular stomatitis virus (VSV) used in this study is an RNA virus, which is easily engineered

Grant sponsor: Japan Society for the Promotion of Science; Grant number: 17K10970.

Correspondence to: Tadahiko Kubo (T: +81-82-257-5232; F: +81-82-257-5234; E-mail: kubot@hiroshima-u.ac.jp)

© 2019 Orthopaedic Research Society. Published by Wiley Periodicals, Inc.

to develop new generations of VSV vectors. Besides VSV, other tumor-specific RNA viruses include reovirus,¹⁹ measles virus,²⁰ poliovirus,²¹ and vaccinia virus.²² Of these viruses, all except VSV have the potential to cause severe human symptoms, whereas VSV rarely infects humans and manifests as mild flu-like symptoms.²³ VSV is sensitive to the interferon response and is tumor-specific owing to the deficiency of antiviral interferon signaling pathways in tumor cells.^{24–26} Deficiency of antiviral interferon signaling in the tumor cells is not provided by other oncolytic viruses. For example, oncorine, which was genetically modified adenovirus, and the very similar Onyx-15 have been engineered to remove a viral defense mechanism that interacts with a normal human gene, p53, that is very frequently dysregulated in cancer cells.²⁷ Furthermore, the time from infection to cytolysis is particularly rapid for VSV, with the viral load increasing by approximately 1000-fold within 24 h.²⁸ Our previous study has shown VSV gene expression, replication, and cytotoxic effects in osteosarcoma cells, but not normal cells.²⁹ The recombinant VSV carrying the near-infrared (NIR) fluorescent protein, Katushka (rVSV-K) is expected to be taken up by all tumor cells and emit intense fluorescence which enable visualization of tumors and complete wide resection.

The purpose of this research is to evaluate the specificity of rVSV-K in osteosarcoma cells and to assess complete tumor resection by rVSV-K fluorescence guidance.

METHODS

Cell Lines and Culture Conditions

Highly metastatic mouse osteosarcoma LM8 cells were obtained from the Cell Engineering Division of Riken Bio-Resource Center (Tsukuba, Ibaraki, Japan). LM8 is a variant of a murine osteosarcoma cell line established by Asai et al. in accordance with the Fidler's method.³⁰ Human osteosarcoma MG-63 and Saos-2 cells were obtained from the American Type Culture Collection (ATCC; Manassas, VA) and cultured in Dulbecco's modified Eagle's medium (DMEM; Wako Pure Chemical Industries, Ltd., Osaka, Japan) supplemented with 10% fetal bovine serum (Gibco, Carlsbad, CA) and 1% penicillin-streptomycin (Wako) at 37°C in a fully humidified incubator under an atmosphere of 5% CO₂. Bone marrow-derived mesenchymal stem cells (BMSCs) were obtained from a 56-year-old male during hip surgery and cultured in Mesenchymal Stem Cell Basal Medium (Lonza Japan, Ltd., Chiba, Japan). Isolation and in vitro expansion of the BMSCs were established as described previously.³¹ BHK-21 cells (ATCC; CCL-10) used for construction and titration of VSV were maintained in DMEM with 10% fetal bovine serum (Gibco).

Virus Generation

Recombinant VSV-K was generated using an established reverse genetics method.^{32,33} Briefly, the Katushka reporter gene was cloned into the *Xho*I and *Nhe*I restriction sites of the plasmid pVSV-XN2, which contains the entire VSV genome sequence (Indiana serotype, GenBank accession number NC_001560) flanked by the T7 promoter, the hepa-

tis delta ribozyme, and the T7 terminator. The plasmid contains *Xho*I and *Nhe*I restriction sites between the G and L genes, flanked by the VSV transcription start and stop signals for insertion of an additional gene.³⁴ The resultant plasmid was transfected into BHK-21 cells constitutively expressing T7 RNA polymerase as well as the helper plasmids pIRES-N, pIRES-P, and pIRES-L to establish a newly recombinant virus, VSV-K^{35,36} (Fig. 1a). Recombinant VSV encoding enhanced GFP (rVSV-GFP) was also generated.³⁴ The viral titers of the stock solution (median tissue culture infective dose [TCID₅₀]/mL) were determined with a standard TCID₅₀ assay using BHK-21 cells.³⁶ Western blot analysis of rVSV-K- and rVSV-GFP-infected BHK21 cell lysate was performed with antibodies against rVSV-K and GFP to confirm the expression of each protein as described previously³⁷ (Fig. 1b).

In Vitro rVSV-K Infection Assays

For virus infection, 3×10^5 cells/well were incubated overnight in six-well plates and then infected with rVSV-K at 10^{-4} or 1 multiplicity of infection (MOI). At 24 h after infection, the cells were evaluated for NIR fluorescent protein expression by fluorescence microscopy (BZ-9000 microscope; Keyence Corporation, Osaka, Japan). Three independent experiments were performed.

Osteosarcoma Mouse Model

The study protocols involving animals were approved by the Ethics Committee for Experimental Animals of Hiroshima University and were performed in strict accordance with the committee guidelines. Inbred C3H male mice, aged 5–6 weeks, were purchased from Shimizu Laboratory Supplies Co., Ltd. (Kyoto, Japan). For the in vivo experiment, LM8 cells (1×10^7 cells per 200 μ l of DMEM) were injected into the subcutaneous tissue of the backs of the mice on day 0 to produce an osteosarcoma animal model. At 2–3 weeks after LM8 administration, the tumor diameters were >1 cm.

In Vivo Fluorescence Labeling of Subcutaneous Tumor

Osteosarcoma mouse models were randomly assigned to one of three different administration groups ($n = 6$ per group) as follows: The rVSV-K group, the rVSV-GFP group, and the saline (control) group. On day 17, mice in the rVSV-K and rVSV-GFP groups received a single intratumoral injection of rVSV-GFP or rVSV-K at 1×10^8 plaque-forming units per 200 μ l. Mice in the saline group received a single intratumoral injection of saline (200 μ l). After injection of rVSV-K or rVSV-GFP, the fluorescence intensity was quantified every day for 7 days using a fluorescence bioimaging system (Night Owl LB983; Berthold Technologies GmbH & Co. KG, Bad Wildbad, Germany) equipped with a Katushka or GFP filter. The fluorescence intensity of the saline (control) group was quantified using a GFP filter.

In addition, the ratio of the fluorescent areas to tumor areas was evaluated. The fluorescent areas of the rVSV-K and rVSV-GFP group ($n = 6$ per group) were calculated using a fluorescence bioimaging system (Night Owl LB983). The tumor areas were calculated in each group using the ellipsoidal formula: Area (m^2) = πab , where "a" and "b" are the major and minor diameters of the tumor, respectively.

Tumor Resection

Osteosarcoma-bearing mice were assigned at random to one of three different resection groups ($n = 6$ per group) as

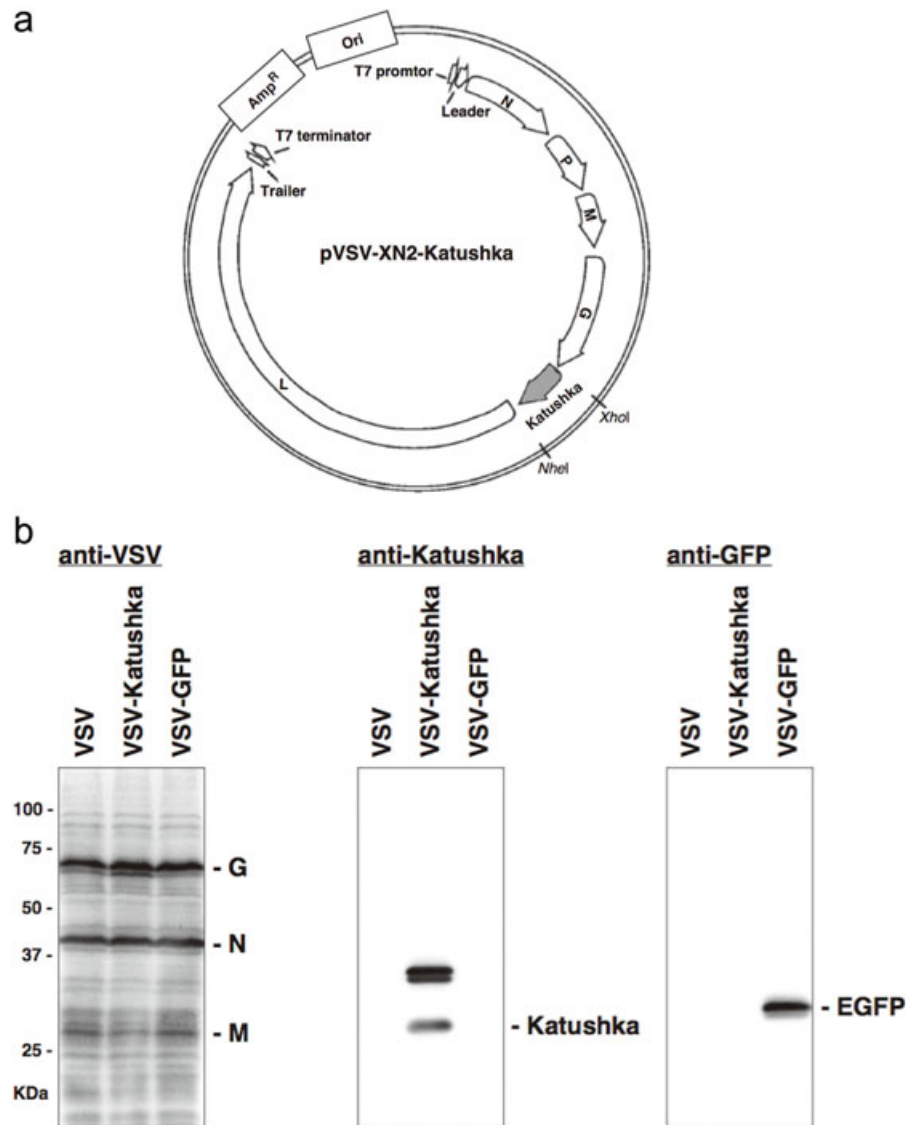


Figure 1. (a) Schematic drawing of pVSV-XN2-Katushka. The VSV Indiana genomic DNA possessing the Leader and Trailer sequences and the N, P, M, G, and L genes is flanked by T7 promoter and T7 terminator. The Katushka cDNA is inserted between the G and L genes by using the *NheI* and *XhoI* restriction sites. (b) Protein expression by rVSVs. BHK21 cells were infected with rVSV-K, rVSV-GFP and the wild-type VSV at a MOI of 10, and cell lysates were prepared at 24 h post-infection. Proteins were analyzed by sodium dodecyl sulfate-polyacrylamide gel electrophoresis and processed for Western blotting by using the indicated antibodies.

follows: The fluorescence-guided resection with rVSV-K (FGR with rVSV-K) group, the non-guided resection with VSV (NGR with VSV) group and the non-guided resection with saline (NGR with saline) group. On day 17 after tumor implantation, mice in the FGR with rVSV-K group received a single intratumoral injection of rVSV-K at 1×10^8 plaque-forming units per 200 μ l, NGR with VSV group received a single intratumoral injection of VSV at 1×10^8 plaque-forming units per 200 μ l, whereas the NGR with saline group received a single intratumoral injection of saline (200 μ l). In FGR with rVSV-K group, recombinant VSV conferred NIR fluorescence to the primary tumor cells. At 24 h after intratumoral injection of rVSV-K, mice were anesthetized with isoflurane, and fluorescence illumination was evaluated using a bioimaging system (Night OWL LB983) equipped with a Katushka filter. The distance between the fluorescent area and the tumor edge was determined using the bioimaging system IndiGo version

2.0.4.0, and the margin of the fluorescent area was marked on the mouse. In the field indicating the fluorescence, tumor with skin as well as the tissue between tumor and retroperitoneum were subsequently resected. In NGR with VSV resection group and NGR with saline group, the tumors were resected at 24 h after intratumoral injection of VSV and saline, respectively. Mice in both groups were anesthetized with isoflurane, and skin incision of tumor margin was macroscopically designed. Tumors with skin and tissue between the tumor and the retroperitoneum were then resected. In each group, the skin was closed with a 6-0 suture.

Upon the death of the mice, tissue suspected as local recurrence (e.g., mass lesion) and tissue around the incision site as well as the lungs were resected. All fluorescent tissues, resected tissues and the lungs were evaluated histologically. In separate experiment, survival rate of the three groups were evaluated.

Histological Analysis

Resected tumors were processed with reference to the cross-sectioning trimming method that is the most commonly used for the first-time removal of small or moderately-sized mass.³⁸ The tumor specimens were fixed in 4% paraformaldehyde overnight and bisected through its shortest axis. Then, each half of the tissue was bisected through its longest axis, creating quarter sections each demonstrating the mass in a different plane, and embedded in paraffin. The tumor specimens were cut at a thickness of 5 μm and then subjected to either hematoxylin and eosin (H&E) staining or immunohistochemical analysis using a monoclonal antibody against the VSV-G protein (VSV11-M; Alpha Diagnostic International, Inc., San Antonio, TX). For immunohistochemical analysis, the sections were counterstained with hematoxylin. The resected tissues, and lungs were fixed in 4% paraformaldehyde overnight and then embedded in paraffin. The samples were cut at a thickness of 5 μm and then subjected to H&E staining.

The distance between the surgical and tumor margins of the histological specimens ($n = 6$ per group) was measured by examining the H&E staining pattern using a Keyence BZ-9000 microscope. In this study, there were four sections for one tumor, among them the site of closest approach of tumor

to the surgical margin on the lateral side was determined and the distance was measured using BZ-II Analyzer software version 1.42. Specimen with a distance of 0 mm was referred to as surgical margin-positive. Local recurrence of the resected tissues ($n = 6$ per group) was then evaluated. Specimen with a visible tumor nodule by H&E staining was referred to as local recurrence-positive. Furthermore, the incidence of lung metastasis in the three groups ($n = 6$ per group) was evaluated.

Statistical Analysis

The peak fluorescence, the ratio of the fluorescent area to the tumor area, and the distance between the surgical and tumor margins were compared either with Student's *t*-test or one-way analysis of variance (ANOVA). The Pearson's chi-square test was used to compare the surgical margin and the local recurrence. Survival curves of the three groups were plotted according to the Kaplan–Meier method. The survival rates were compared using the log-rank test. All analyses were performed using IBM SPSS Statistics for Windows, version 22.0 (IBM Corporation, Armonk, NY). Values are presented as the mean \pm standard deviation (SD). A probability (*p*) value of <0.05 was considered statistically significant.

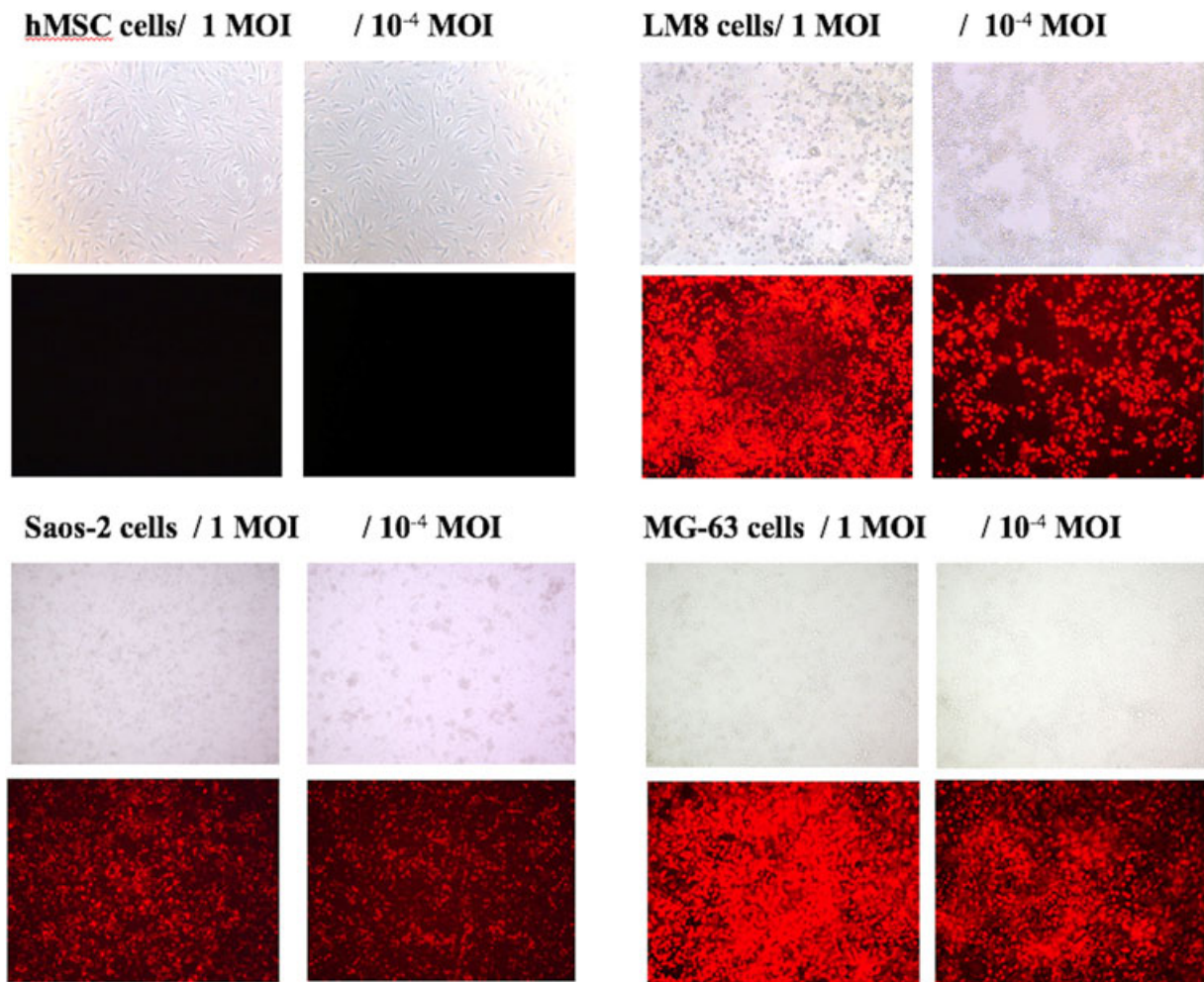


Figure 2. NIR fluorescence expression in vitro. Mouse (LM8) and human (Saos-2 and MG-63) osteosarcoma cells and normal human BMSCs were infected with rVSV-K at a MOI of 1 and 10^{-4} . NIR fluorescence was observed only in osteosarcoma cells (LM8, Saos-2, and MG-63) even at low-concentration infections.

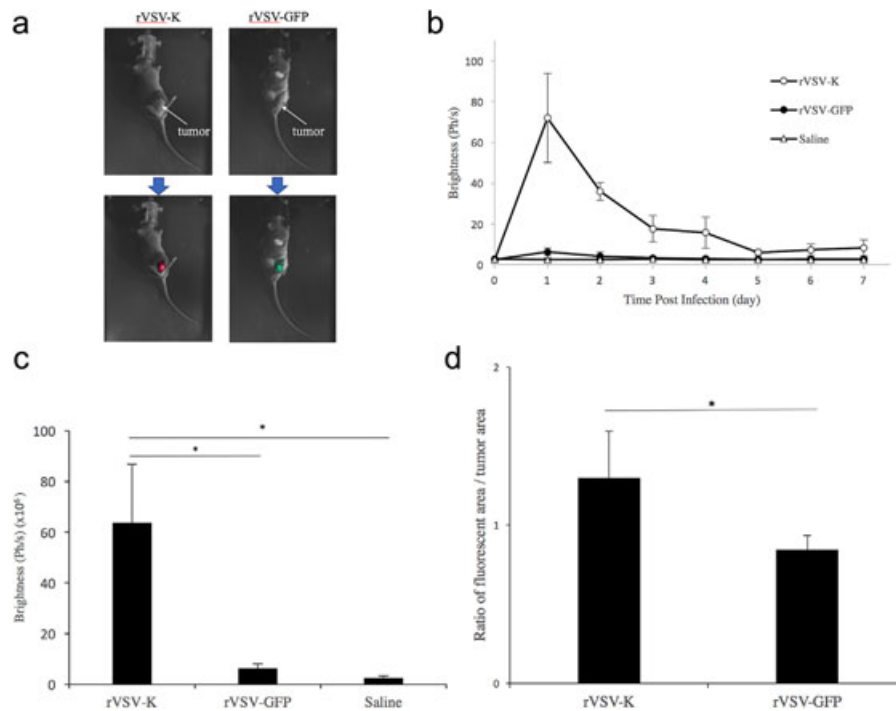


Figure 3. (a) Fluorescent image obtained by the fluorescence bioimaging system. The fluorescent image obtained by the fluorescence bioimaging system. Representative images of tumors infected with rVSV-K (left) and rVSV-GFP (right). (b) Evaluation of tumor fluorescence intensity. The fluorescence intensities of the rVSV-K, rVSV-GFP, and saline (control) groups were evaluated at the indicated times. The vertical axis indicates the average amount of fluorescence in the fluorescent area (Ph/s). Data are presented as the mean \pm SD obtained from six mice per group. The peak amount of fluorescence was at 1 day after the rVSV-K or rVSV-GFP injection. (c) The peak fluorescence intensity. Fluorescence intensity was greater in the rVSV-K group than in the other two groups. Data are presented as the mean \pm SD obtained from six mice per group. * $p < 0.05$ (ANOVA). (d) The ratio of the fluorescent area to tumor area was significantly greater in the rVSV-K group than in the rVSV-GFP group. Data are presented as the mean \pm SD obtained from six mice per group. * $p < 0.05$ (Student's *t*-test).

RESULTS

In Vitro rVSV-K Specificity for Osteosarcoma Cells

Mouse osteosarcoma LM8 cells, but not human BMSCs, showed NIR fluorescence expression by infection with even a low concentration of rVSV-K. The results of the human osteosarcoma Saos-2 and MG-63 cells were similar (Fig. 2). These results indicate that rVSV-K is specific to osteosarcoma cells and that the time from infection to spread is rapid.

Fluorescence Intensity of Osteosarcoma by Injection In Vivo With VSV

Representative images of tumors in the rVSV-K and rVSV-GFP groups captured with the bioimaging system are shown in Fig. 3a. NIR and GFP fluorescence expression was observed in mice administered with rVSV-K and rVSV-GFP, respectively. Fluorescence was not visually observed in mice administered with saline (data not shown). The results of the fluorescence intensity for 7 days are shown in Fig. 3b. In the rVSV-K group, there was a rapid increase in fluorescence on day 1, which subsequently decreased. Fluorescence peaked on day 1 in the rVSV-K and rVSV-GFP groups. The intensity of the peak fluorescence was statistically greater in the rVSV-K group than in the rVSV-GFP and saline (control) groups ($p < 0.05$, ANOVA; Fig. 3c).

The Ratio of Fluorescent Area and Tumor Area

The ratio of the fluorescent area to tumor area was evaluated. The average ratio of the fluorescent area to tumor area was significantly greater in the rVSV-K group than in the rVSV-GFP group (1.30 vs. 0.84, respectively, $p < 0.05$, Student's *t*-test; Fig. 3d). The rVSV-GFP was not suitable for fluorescence-guided resection of a subcutaneous osteosarcoma because GFP fluorescence expression was not induced in all tumor margins. Based on these findings, fluorescent resection was performed in the rVSV-K-guided resection group.

Fluorescence-guided Resection With rVSV-K

A representative specimen that shows distance between the surgical and tumor margins is shown in Fig. 4a. The average distance between the surgical and tumor margins was significantly greater in the FGR with rVSV-K group than in the NGR groups with either VSV or saline ($p < 0.05$, ANOVA; Fig. 4b). Microscopic invasion was observed in three tumor specimens in the FGR with rVSV-K group (Fig. 4c), whereas no microscopic invasion was observed in the NGR with VSV group and NGR with saline group. These results show that FGR with rVSV-K enabled tumor wide resection. Three tumor specimens in each NGR group had positive surgical margins. Conversely,

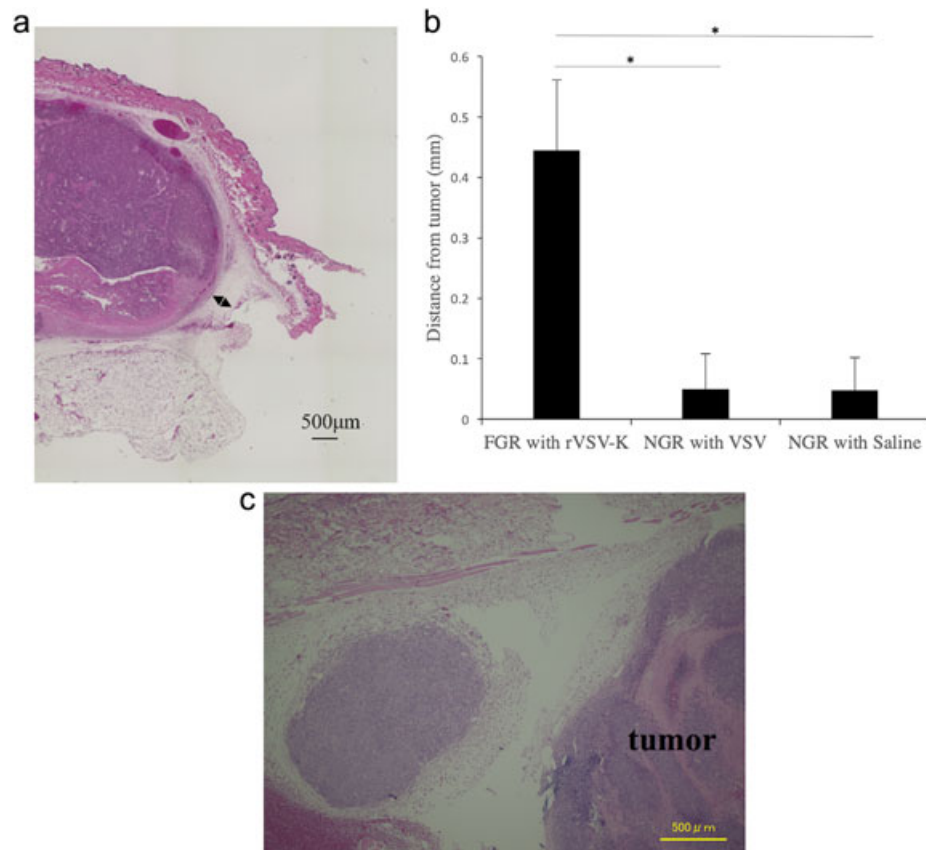


Figure 4. (a) A representative specimen of the resected tumor. The bidirectional arrow shows the distance between the surgical and tumor margins. (b) The distance between the surgical and tumor margins was significantly larger in the FGR with rVSV-K group than in the NGR groups. Data are presented as the mean \pm SD obtained from six mice per group. * $p < 0.05$ (ANOVA). (c) A representative specimen which indicated microscopic invasion in the FGR with rVSV-K group. A small tumor nodule was present adjacent to the primary tumor.

none of the specimens in the FGR with rVSV-K group had a positive surgical margin. The surgical margin rate was significantly lower in the FGR with rVSV-K group than in NGR groups with either VSV ($p = 0.046$, Pearson's chi-square test) or saline ($p = 0.046$, Pearson's chi-square test; Table 1). These findings suggest that NGR with VSV and NGR with saline may fail to resect microscopic invasion. Tumor lesions in the FGR with rVSV-K group and in the NGR with VSV group showed positive for VSV-G protein (Fig. 5a), but not in the NGR with saline group (Fig. 5b). These results indicate that VSV successfully infected the primary tumor after intratumoral administration of the virus.

Local Recurrence

Three tissue sections in NGR with VSV group and three tissue sections in NGR with saline group that originated from mice with positive surgical margins contained a tumor mass or nodule around the incision site. In contrast, none of the sections in the FGR with rVSV-K group had a tumor nodule. The local recurrence rate was significantly lower in the FGR with rVSV-K group than in NGR groups with either VSV ($p = 0.046$, Pearson's chi-square test) or saline ($p = 0.046$, Pearson's chi-square test; Table 2).

Distant Metastasis and Survival Rate

All lung specimens of the three groups had metastatic nodules. The distant metastasis rate was 100% in all groups. The average survival time after injection of LM8 cells in the FGR with rVSV-K group, NGR with VSV group and NGR with saline group were 40, 37, and 35.5 days respectively. A comparison of the Kaplan–Meier survival curves showed that survival was longer in the FGR with rVSV-K group than in the NGR groups, but this difference was not statistically significant ($p = 0.371$, log-rank test; Fig. 6).

DISCUSSION

Our previous study has shown that arterial injection of VSV into rats with osteosarcoma resulted in the inhibition of tumor growth and VSV targeting of the

Table 1. Surgical Margin After the FGR With rVSV-K, NGR With VSV and NGR With Saline

Surgical margin	Positive	Negative
FGR with rVSV-K	0	6
NGR with VSV	3	3
NGR with saline	3	3

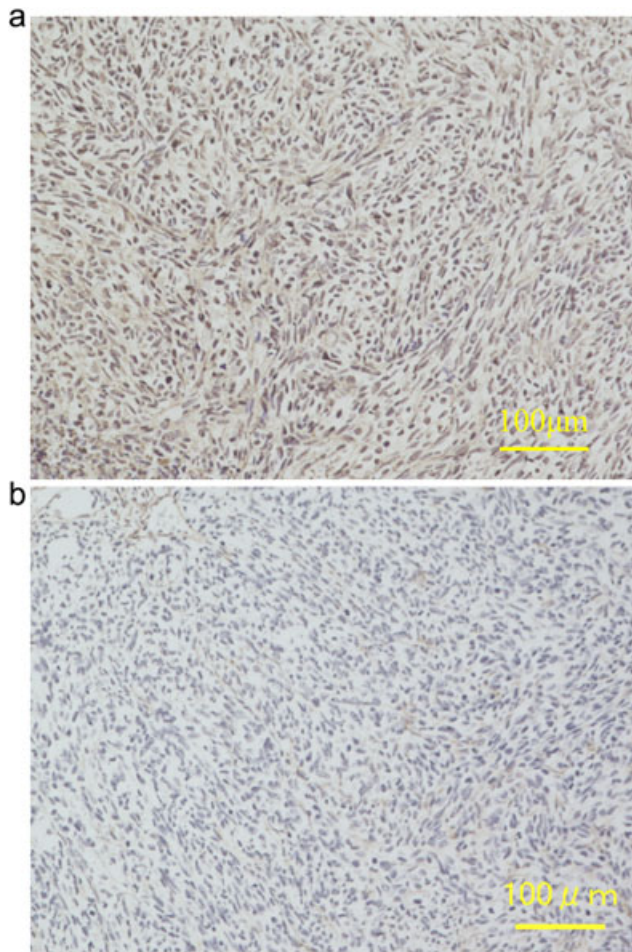


Figure 5. (a) A representative immunostaining specimen either of the FGR with rVSV-K or NGR with VSV. Immunohistological brown staining was performed using a monoclonal antibody against the VSV-G protein ($\times 100$, magnification). (b) A representative immunostaining specimen of the NGR with saline. Immunohistological brown staining was performed using a monoclonal antibody against the VSV-G protein ($\times 100$, magnification).

tumor.²⁹ Few studies have demonstrated that VSV is specific to sarcoma cells.^{26,29,39} In this study, VSV transfected a wide range of osteosarcoma cells even at low concentrations, but it did not detectably transfect human BMSCs. Therefore, VSV is thought to be highly suitable for use as a vector of a fluorescent substance to target osteosarcoma cells.

Katushka protein, first reported by Shcherbo et al. in 2007,⁴⁰ was used in this study as a fluorescence bioimaging. The protein emits light in the NIR wavelength ranges with excitation and emission spectra

peak at 588 and 635 nm, respectively.⁴⁰ NIR wavelengths are able to penetrate the body for several millimeters.⁴¹ Katushka protein does not aggregate with other toxic elements in the cell⁴² and has strong fluorescence,^{40,42} which is necessary for visualization of the tumor margin for complete wide resection.

Among previous reports of the use of fluorescence bioimaging in tumor resection, Kishimoto et al. incorporated GFP into a telomerase-dependent adenovirus for fluorescence bioimaging during colorectal cancer resection.¹⁵ Yano et al. used fluorescence bioimaging with GFP incorporated into a telomerase-dependent adenovirus in colon cancer and osteosarcoma resection, and found that the local recurrence rate had decreased as compared with marginal resection.^{16–18} Miwa et al. used RFP (DsRed-2)-expressing osteosarcoma (143B) cells for fluorescence-guided surgery of a nude mouse model of osteosarcoma.⁴³ In the present study, the fluorescence intensity and ratio of the fluorescent areas to tumor areas were compared between the rVSV-K and rVSV-GFP groups. In the rVSV-K group, the fluorescent area was larger than the tumor margin. This could be due to the statistically stronger fluorescence by rVSV-K extended from the tumor itself as was shown in our study when comparing with that of rVSV-GFP. Furthermore, microscopic invasion was found on tumor specimens of the FGR with rVSV-K group. This finding suggests a contribution of microscopic invasion as the tumor cells beyond the main tumor edge to the observed larger fluorescent area, which was resected along with primary tumor by rVSV-K guidance technique.

VSV-Katushka used in our preclinical study emits NIR wavelengths. A previous clinical study has demonstrated that, NIR fluorescence image-guided surgery could identify small cancer nodules, which were not visible by preoperative CT.⁴⁴ This system showed the potential ability to ensure the real-time removal of small tumor nodules that could be missed during surgery. NIR fluorescence imaging approach is being developed to improve imaging depth as well as the quality of the resolution images. A previous study has shown the depth to be approximately 5–15 mm.⁴⁵ To address this issue, a combination of radioactive tracers and NIR fluorescence, which is used for cancer,^{46,47} might be developed for deep tissue tumors such as osteosarcoma.

Obtaining sufficient margins is not relatively easy in osteosarcoma of the spine, and in such cases it is unclear how fluorescence-guided tumor wide resection would substantially aid surgical resection as the primary difficulty is not visualization of the tumor margins. In our study, we showed complete wide resection of osteosarcoma implanted subcutaneously could be achieved by rVSV-K guided approach. These findings warrant further studies using other osteosarcoma mouse models, including osteosarcoma of the spine to better evaluate the feasibility of rVSV-K approach to achieve completed surgical resection.

Table 2. Local Recurrence After the FGR With rVSV-K, NGR With VSV and NGR With Saline

Local recurrence	Positive	Negative
FGR with rVSV-K	0	6
NGR with VSV	3	3
NGR with saline	3	3

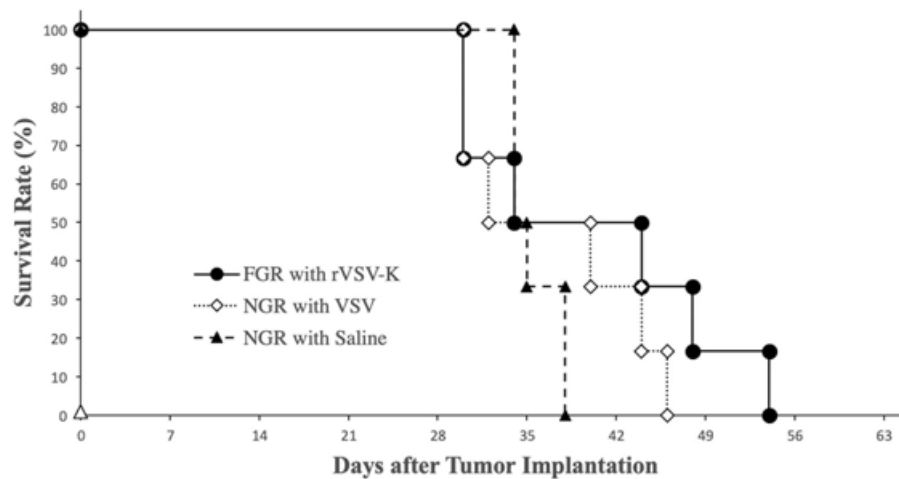


Figure 6. Kaplan–Meier survival curves of the three resection groups. There was no significant difference between the three groups, as shown by the log-rank test: $p = 0.371$.

Few studies have demonstrated an exceptionally low local recurrence rate after resection. In the present study, the local recurrence rate was not found in the FGR with rVSV-K group. A possible reason for this result might be related to the fact that complete tumor resection in the FGR with rVSV-K group included microscopic tumor nodules. In the NGR with VSV group, such nodules existed even after resection, which might cause local recurrence. These findings suggest that the reduced local recurrence is not due to virus-mediated oncolysis but due to guidance technique. This study is the first to report that intratumoral administration of rVSV-K was able to emit intense fluorescence in primary osteosarcoma tumor allowing for complete osteosarcoma-wide resection.

In this study, although mice in the FGR with rVSV-K group tended to survive for a longer period than those in the NGR groups, there were no significant differences statistically, and distant metastasis occurred in all groups. Reddy et al. reported that no difference was observed in survival outcome between limb salvage surgery with local recurrence and initial amputation without local recurrence.⁷ Whether local recurrence correlates with survival outcome in osteosarcoma patients is still controversial. Another study has found an association of positive margins with overall survival in high-grade osteosarcoma patients.⁸ Bertrand et al. conducted a study including 241 patients and found that patients with positive margins had a higher probability of local recurrence, and had the worse survival outcome at 2 years follow-up than those with negative margins. Interestingly, in their 46 negative-margin patients, 13 experienced metastasis and 10 died during the follow-up period. They did admit several limitations to their study that could have influenced the impact of the conclusion, including a remarkable number of patients not followed-up, a small sample size, and short period of follow-up, all factors which may not allow for long-term survival evaluation.⁸ In our study, no significant survival

difference between all groups might be due to the high metastatic characteristics of LM8 cells in vivo,^{30,48} in which circulating tumor cells (micrometastasis) might be present before tumor resection was performed. Metastasis and survival might be due to micrometastasis existing prior to resection that occurs in approximately 80% of osteosarcoma patients, including almost all who succumb to their disease.⁴⁹ Furthermore, only a small proportion of the patients with metastases and poor prognosis have local recurrence. Therefore, metastasis and survival would not be affected by our surgical technique. These findings indicate that although FGR with rVSV-K can prevent local recurrence, it does not prevent distant metastasis. The appropriate surgical strategy is not for systemic control but for local control. Previous reports using VSV as systemic therapy in experimental osteosarcoma metastases have reported survival prolongation in vivo.³⁶ These data suggest further development of the new comprehensive approach of fluorescence-guided resection combined with systemic virotherapy by using VSV which may enhance osteosarcoma management to prevent local recurrence and metastasis, thus prolonging survival.

In conclusion, the results of this study demonstrated that rVSV-K selectively infected osteosarcoma cells both in vitro, and that NIR fluorescence bioimaging with rVSV-K enables easy visualization of primary tumor margins which enable complete wide resection. A fluorescence bioimaging system using rVSV-K might be very useful for complete tumor resection.

AUTHORS' CONTRIBUTIONS

TS, TK, MO, and NA are responsible for study concepts and design. TS, MPJ, TF, TS, and MN are responsible for data acquisition, analysis, and interpretation. TS, TK, MPJ, TF, TS, MN, MO, and NA are responsible for drafting and proofreading of the manuscript. TS, TK, MPJ, TF, TS, MN, MO, and NA are

responsible for final approval of the manuscript for publication. All authors have made a significant contribution to this manuscript, approved the final manuscript, and agreed with this submission to the *Journal of Orthopaedic Research*.

ACKNOWLEDGMENTS

This study was supported by a grant from the Japan Society for the Promotion of Science (grant no. 17K10970). The funding organization played no role in the study design, data collection/analysis, decision to publish, or preparation of the manuscript.

REFERENCES

- Rosen G. 1985. Preoperative (neoadjuvant) chemotherapy for osteogenic sarcoma: a ten year experience. *Orthopedics* 8:659–664.
- Allison DC, Carney SC, Ahlmann ER, et al. 2012. A meta-analysis of osteosarcoma outcomes in the modern medical era. *Sarcoma* 2012:704872.
- Marcove RC, Abou-Zahr K. 1984. En block surgery for osteogenic sarcoma: analysis and review of ninety operative cases. *Bull NY Acad Med* 60:748–758.
- He F, Zhang W, Shen Y, et al. 2016. Effects of resection margins on local recurrence of osteosarcoma in extremity and pelvis: systematic review and meta-analysis. *Int J Surg* 36:283–292.
- Weeden S, Grimer RJ, Cannon SR, et al. 2001. The effect of local recurrence on survival in resected osteosarcoma. *Eur J Cancer* 37:39–46.
- Dekutoski MB, Clarke MJ, Rose P, et al. 2016. Osteosarcoma of the spine: prognostic variables for local recurrence and overall survival, a multicenter ambispective study. *J Neuros Spine* 25:59–68.
- Reddy KI, Wafa H, Gaston CL, et al. 2015. Does amputation offer any survival benefit over limb salvage in osteosarcoma patients with poor chemonecrosis and close margins? *Bone Joint J* 97-b:115–120.
- Bertrand TE, Cruz A, Binitie O, et al. 2016. Do surgical margins affect local recurrence and survival in extremity, nonmetastatic, high-grade osteosarcoma? *Clin Orthop Relat Res* 474:677–683.
- Tipirneni KE, Rosenthal EL, Moore LS, et al. 2017. Fluorescence imaging for cancer screening and surveillance. *Mol Imag Biol* 19:645–655.
- Moore GE, Peyton WT. 1948. The clinical use of fluorescein in neurosurgery; the localization of brain tumors. *J Neuros* 5:392–398.
- Kain SR, Adams M, Kondepudi A, et al. 1995. Green fluorescent protein as a reporter of gene expression and protein localization. *BioTechniques* 19:650–655.
- Craandijk A, Van Beek CA. 1976. Indocyanine green fluorescence angiography of the choroid. *Bri J Ophthalmol* 60:377–385.
- Inoue Y, Izawa K, Yoshikawa K, et al. 2007. In vivo fluorescence imaging of the reticuloendothelial system using quantum dots in combination with bioluminescent tumour monitoring. *Eur J Nucl Med Mol Imag* 34:2048–2056.
- Adusumilli PS, Stiles BM, Chan MK, et al. 2006. Real-time diagnostic imaging of tumors and metastases by use of a replication-competent herpes vector to facilitate minimally invasive oncological surgery. *FASEB J* 20:726–728.
- Kishimoto H, Zhao M, Hayashi K, et al. 2009. In vivo internal tumor illumination by telomerase-dependent adenoviral GFP for precise surgical navigation. *Proc Natl Acad Sci USA* 106:14514–14517.
- Yano S, Takehara K, Miwa S, et al. 2016. Improved resection and outcome of colon-Cancer liver metastasis with fluorescence-Guided surgery using In situ GFP labeling with a telomerase-Dependent adenovirus in an orthotopic mouse model. *PLoS ONE* 11:e0148760.
- Yano S, Miwa S, Kishimoto H, et al. 2016. Eradication of osteosarcoma by fluorescence-guided surgery with tumor labeling by a killer-reporter adenovirus. *J Orthop Res* 34:836–844.
- Yano S, Miwa S, Kishimoto H, et al. 2015. Targeting tumors with a killer-reporter adenovirus for curative fluorescence-guided surgery of soft-tissue sarcoma. *Oncotarget* 6:13133–13148.
- Zhao X, Chester C, Rajasekaran N, et al. 2016. Strategic combinations: the future of oncolytic virotherapy with reovirus. *Mol Cancer Therap* 15:767–773.
- Robinson S, Galanis E. 2017. Potential and clinical translation of oncolytic measles viruses. *Expert Opin Biol Ther* 17:353–363.
- Denniston E, Crewdson H, Rucinsky N, et al. 2016. The practical consideration of poliovirus as an oncolytic virotherapy. *Am J Virol* 5:1–7.
- Wang H, Chen NG, Minev BR, et al. 2013. Optical detection and virotherapy of live metastatic tumor cells in body fluids with vaccinia strains. *PLoS ONE* 8:e71105.
- Letchworth GJ, Rodriguez LL, Del cbarrera J. 1999. Vesicular stomatitis. *Vet J* 157:239–260.
- Obuchi M, Fernandez M, Barber GN. 2003. Development of recombinant vesicular stomatitis viruses that exploit defects in host defense to augment specific oncolytic activity. *J Virol* 77:8843–8856.
- Stojdl DF, Lichty B, Knowles S, et al. 2000. Exploiting tumor-specific defects in the interferon pathway with a previously unknown oncolytic virus. *Nat Med* 6:821–825.
- Paglino JC, van den Pol AN. 2011. Vesicular stomatitis virus has extensive oncolytic activity against human sarcomas: rare resistance is overcome by blocking interferon pathways. *J Virol* 85:9346–9358.
- Garber K. 2006. China approves world's first oncolytic virus therapy for cancer treatment. *J Natl Cancer Inst* 98:298–300.
- Huang TG, Ebert O, Shinozaki K, et al. 2003. Oncolysis of hepatic metastasis of colorectal cancer by recombinant vesicular stomatitis virus in immune-competent mice. *Mol Ther* 8:434–440.
- Kubo T, Shimose S, Matsuo T, et al. 2011. Oncolytic vesicular stomatitis virus administered by isolated limb perfusion suppresses osteosarcoma growth. *J Orthop Res* 29:795–800.
- Asai T, Ueda T, Itoh K, et al. 1998. Establishment and characterization of a murine osteosarcoma cell line (LM8) with high metastatic potential to the lung. *Int J Cancer* 76:418–422.
- Kotobuki N, Hirose M, Takakura Y, et al. 2004. Cultured autologous human cells for hard tissue regeneration: preparation and characterization of mesenchymal stem cells from bone marrow. *Artif Organs* 28:33–39.
- Lawson ND, Stillman EA, Whitt MA, et al. 1995. Recombinant vesicular stomatitis viruses from DNA. *Proc Natl Acad Sci USA* 92:4477–4481.
- Whelan SP, Ball LA, Barr JN, et al. 1995. Efficient recovery of infectious vesicular stomatitis virus entirely from cDNA clones. *Proc Natl Acad Sci USA* 92:8388–8392.
- Ebert O, Shinozaki K, Huang TG, et al. 2003. Oncolytic vesicular stomatitis virus for treatment of orthotopic hepatocellular carcinoma in immune-competent rats. *Cancer Res* 63:3605–3611.

35. Nishimura K, Sano M, Ohtaka M, et al. 2011. Development of defective and persistent Sendai virus vector: a unique gene delivery/expression system ideal for cell reprogramming. *J Biol Chem* 286:4760–4771.
36. Johan MP, Kubo T, Furuta T, et al. 2018. Metastatic tumor cells detection and anti-metastatic potential with vesicular stomatitis virus in immunocompetent murine model of osteosarcoma. *J Orthop Res*.
37. Irie T, Shimazu Y, Yoshida T, et al. 2007. The YLDD sequence within Sendai virus M protein is critical for budding of virus-like particles and interacts with Alix/AIP1 independently of C protein. *J Virol* 81:2263–2273.
38. Kamstock DA, Ehrhart EJ, Getzy DM, et al. 2011. Recommended guidelines for submission, trimming, margin evaluation, and reporting of tumor biopsy specimens in veterinary surgical pathology. *Vet Pathol* 48:19–31.
39. Abdelbary H, Brown CW, Werier J, et al. 2014. Using targeted virotherapy to treat a resistant Ewing sarcoma model: from the bedside to the bench and back. *Sci World J* 2014:171439.
40. Shcherbo D, Merzlyak EM, Chepurnykh TV, et al. 2007. Bright far-red fluorescent protein for whole-body imaging. *Nat Methods* 4:741–746.
41. Kuchimaru T, Iwano S, Kiyama M, et al. 2016. A luciferin analogue generating near-infrared bioluminescence achieves highly sensitive deep-tissue imaging. *Nat Commun* 7:11856.
42. Hoffman RM. 2008. A better fluorescent protein for whole-body imaging. *Trends Biotechnol* 26:1–4.
43. Miwa S, Hiroshima Y, Yano S, et al. 2014. Fluorescence-guided surgery improves outcome in an orthotopic osteosarcoma nude-mouse model. *J Orthop Res* 32:1596–1601.
44. Satou S, Ishizawa T, Masuda K, et al. 2013. Indocyanine green fluorescent imaging for detecting extrahepatic metastasis of hepatocellular carcinoma. *J Gastroenterol* 48: 1136–1143.
45. Mondal SB, Gao S, Zhu N, et al. 2014. Real-time fluorescence image-guided oncologic surgery. *Adv Cancer Res* 124:171–211.
46. van der Poel HG, Buckle T, Brouwer OR, et al. 2011. Intraoperative laparoscopic fluorescence guidance to the sentinel lymph node in prostate cancer patients: clinical proof of concept of an integrated functional imaging approach using a multimodal tracer. *Eur Urol* 60: 826–833.
47. Brouwer OR, Buckle T, Vermeeren L, et al. 2012. Comparing the hybrid fluorescent-radioactive tracer indocyanine green-99mTc-nanocolloid with 99mTc-nanocolloid for sentinel node identification: a validation study using lymphoscintigraphy and SPECT/CT. *J Nucl Med* 53:1034–1040.
48. Yui Y, Itoh K, Yoshioka K, et al. 2010. Mesenchymal mode of migration participates in pulmonary metastasis of mouse osteosarcoma LM8. *Clin Exp Metastasis* 27: 619–630.
49. Coventry MB, Dahlin DC. 1957. Osteogenic sarcoma; a critical analysis of 430 cases. *J Bone Joint Surg Am* 39-a:741–757; discussion, 757–748.